Journal of Environmental Sciences Vol. 18, No. 1, pp. 76—82, 2006

ISSN 1001—0742
CN 11—2629/X

Article ID: 1001-0742(2006)01-0076-07 CLC number: X132; O644 Document code: A

Morphology of metal nanoparticles photodeposited on TiO_2/silical gel and photothermal activity for destruction of ethylene

HU Chun*, LIN Lan-yu, HU Xue-xiang

(Research Center for Eco-Environmental Sciences, Chinese Academy of Sciences, Beijing 100085, China. E-mail: huchun@mail.rcees.ac.cn)

Abstract: The morphology of supported metal nanoparticles on TiO_2/silical gel (TSO) and photothermal synergism were investigated for destruction of ethylene. During photocatalytic deposition of metal nanopartilces, the effects of pH and light intensity on the morphology of coated platinum, palladium, gold on TiO_2/silical gel were studied. Moreover, these catalysts were characterized by TEM, UV-Vis DRS. The pH of preparing solution have strong influence on dispersion, size and sites of Pt, Pd and Au on TSO, which were controlled by the electrostatic binding of $HPtCl_6^-$, $AuCl_4^-$ and $TiOH_2^+$, $Pd^{2+}$and TiO^- respectively. Platinum, gold and palladium nanoparticles were uniformly highly dispersed on the titanol sites not silanol of TiO_2 /silical gel under pH=2, pH =9.9 respectively. For the photodegradation of ethylene, they show higher photothermal efficiency than those prepared with other pH conditions under UV illumination in a non-circulating photoreactor. The optimum weight loadings of Pt, Au, and Pd were 0.25 wt%, 0.5 wt%, 1 wt%, respectively. The synergistic effect enhanced ethylene removal and CO_2 production. These results verify that the best photothermal synergistic effect depends on the dispersion, size of noble metal nano-particles. FTIR analyses of the used Pt-, Pd-TSO catalysts indicated that no significant by-products were accumulated on the surface of the catalysts, leading to them longer lifetime.

Keywords: photodeposition; TiO_2/silical gel; noble metal; dispersion; photothermal synergism

Introduction

Photocatalytic oxidation (PCO) is a suitable method for the removal of volatile organic chemicals (VOCs) in enclosed atmospheres(Peral, 1992; Alberici and Jardim, 1995). This technique presents several advantages over other decontamination processes, among which the mild conditions of operation and the lack of specificity regarding the organic target are possibly the most relevant from a practical point of view. Nevertheless, the anatase phase of TiO_2, which is the most widely used photocatalyst, presents certain limitations. Thus, formation of partial oxidation products, some of them very noxious, can occur, especially when dealing with high concentrations of pollutants (Ameen, 1999). Deactivation of the photocatalysts constitutes another important issue that can severely reduce the effectiveness of this method for the removal of certain VOCs during prolonged operation. Therefore, in order to achieve the current environmental requirements further improvement of the characteristics of the photocatalysts is warranted. In this way, different approaches have been adopted to promote the photocatalytic activity of TiO_2, including its preparation as nanosized particles (Yu, 2003), and the incorporation of transition (Fuerte *et al.*, 2001) or noble metals (Fu *et al.*, 1995; Kennedy and Datye, 1998; Vorontsov *et al.*, 1999). It has been reported that the addition of platinum to TiO_2 catalyst improves considerably its performance for the photocatalytic oxidation of different organic chemicals(Einaga *et al.*, 2001; Nosaka *et al.*, 1996). Moreover, the oxidation of VOCs over these catalysts may not be entirely a photo-induced process, because depending on the experimental conditions the noble metal can also catalyze the thermal combustion of the pollutants (Kennedy and Datye, 1998; Vorontsov *et al.*, 1999). As a consequence, a moderate increase in the operation temperature enhances the performance of these systems, and the mineralization of different organic molecules can be fully accomplished. Other precious metals are also effective catalysts for VOCs combustion (Papaefthimiou *et al.*, 1998). Datye *et al.* observed that Pt increased the rate of ethanol PCO, and they observed a significant photothermal synergistic effect (Kennedy and Datye, 1998). The overall conversion on illuminated Pt / TiO_2 was much greater than the sum of conversions for PCO on TiO_2 plus thermal catalytic reaction on Pt. The synergistic effect depended on how the catalysts were prepared. It is anticipated that size and morphology of the metal clusters on a solid support have a profound impact on the activity of the catalyst(Scatter, 1986; Zhang, 1999; Watanabe *et al.*, 1989).

In this study, a simple and straightforward photocatalytic method was employed to deposit metal clusters(Pt, Pd, Au) on the surface of bond-conjugated TiO_2/silica gel (TSO), with a certain degree of control in coating morphology. The key influential factors: pH, photodeposition time, and light intensity will be

Foundation item: The National Natural Science Foundation of China (No. 20377050), and the Hi-Tech Research and Development Program (863) of China(No. 2005AA642030); * Corresponding author

reported. Ethylene is a plant hormone that promotes the ripening of fruits and vegetables and accelerates the aging of flowers. Effects of reaction temperature, water and Pt on photocatalytic oxidation of ethylene have been investigated (Fu *et al.*, 1996; Zorn *et al.*, 2000). Fu *et al.* observed that the fraction of ethylene that reacts is stoichiometrically oxidized to CO_2. Ethylene was selected as model compound to evaluate the effects of the morphology of metal nanoparticles (dispersion state, size) on its photothermal oxidation aiming to obtain the best photothermal activity catalyst. Ti-OH_2^+ and Ti-O^- are the main groups on the surface of TSO under acidic and alkaline conditions, respectively. The dispersion and size of noble metal nanoparticles can be controlled by the electrostatic force between precursor and the two surface groups of TSO. The relationship between preparation of noble metal nanoparticles and activity was discussed in detail.

1 Experimental

1.1 Preparation of TiO_2/silica gel particles

Silica gel (100—200 mesh, Qingdao Chemical Factory, China) was dried and impregnated with cyclohexane solution of $Ti(OC_4H_9)_4$ (chemical purity, Changcheng Chemical Company, Beijing) for 15 h. After the cyclohexane solvent was completely vaporized at 313 K, the silica gel was dried at 393 K for 6 h, and then calcined in the air in three different steps: 473 K for 1 h, 623 K for 1 h, and then 723 K for 8 h. The tested TiO_2/silica gel (TSO) contained 30% wt TiO_2.

1.2 Preparation of M-TiO_2/silical gel (M: Pt, Pd, Au, Ag)

All preparation experiments were carried out in a fluidized bed photoreactor, which consists of a 400 ml cylindrical glass body with gas outlet port and gas inlet at the bottom of the glass body. A 4 W blacklight lamp(365 nm) surrounded by a glass thimble was located in the center of the reactor. In a typical preparation experiment, a suspension of TiO_2/silical gel was first prepared by mixing 2 g TiO_2/silical gel and certain concentration H_2PtCl_6 or $PdCl_2$, or $HAuCl_4$ and 0.1 mol/L methanol aqueous solution with 200 ml water. The suspension was purged with a stream of nitrogen for 30 min and then irradiated with blacklight lamp. pH of the solution was adjusted with HCl or NaOH. After the given irradiation time, the white TSO became dark gray. The suspension was then centrifuged and the supernatant was removed for atomic absorption spectrometry (AAS) analysis. The particles were washed with deionized water to eliminate some ions produced from photodeposition, and then dried at 373 K for 4 h. Thus, Pt-TSO, Pd-TSO, Au-TSO were obtained.

1.3 Characterization

The UV-Vis diffuse reflectance spectra (DRS) of the samples in the wavelength range of 200—800 nm were determined using a spectrophotometer (Hitachi Model U-3100) with 150ϕ integral ball. Transmission electron microscopy (TEM) micrographs were obtained on 120 kV TECNAIG^2 Philips electron microscope. Samples were prepared by depositing aqueous suspensions on 200 mesh copper grids with holey carbon film. DRFTIR spectra of powder sample were recorded by accumulation of 263 scans with a resolution of 4 cm^{-1} in Bruker T27 equipment provided with a MCT detector cooled with liquid N_2. The sample was purged with nitrogen gas at 373 K for 2 h. In the case of adsorption experiments a fixed dose of CO 3% was admitted in the diffuse reflection FTIR cell.

1.4 Photocatalytic experiments

The photodegradation of ethylene was carried out in a non-circulating mode with a flow rate 50 ml/min. Ethylene (1050 mg/L, balance nitrogen) and air(21% oxygen, balance nitrogen), whose flow rates were controlled by mass flow meter, were used as received from compressed gas cylinders. The tested photocatalyst pellets were placed into the glass tube(glass: maximum length 30 cm, diameter 0.65 cm). Four 4 W blacklight lamps (365 nm) surrounded the glass tube. Heat was applied to the outside of the reactor tube with nylon heating tape, and the temperature determined at the axial midpoint by a thermocouple situated the catalyst pellets. The product stream from the reactor was allowed to flow continuously to sampling loop of a chromatographic valve. A gas chromatograph equipped with a catalytic conversion furnace and a flame ionization detector (FID), and a Porapak Q column was employed to analyze discrete samples of the reactor effluent stream. The concentrations of ethylene and carbon dioxide were determined by using the catalytic conversion furnace and FID. The GC was calibrated using known concentrations of ethylene and carbon dioxide.

2 Results and discussion

2.1 Effect of pH on the dispersion of metal

To achieve an optimal synergistic effect, the influence of pH on the morphology metal clusters with desired size and distribution pattern on a given surface area of TiO_2/silica gel(TSO) were examined in detail. Three metal ions precursors, H_2PtCl_6, $PdCl_2$, and

$HAuCl_4$ were selected to investigate the effect of the electrostatic force on the nanosize and dispersion of metal on the surface of TSO. In all cases, the photoreduction of tested metal ions is nearly 100% to the completion. Fig.1a and Fig.1b show transmission electron microscopy (TEM) images of 0.5% Pt-TSO prepared under pH=2 and pH=6.58. Clearly, the former Pt was uniformly dispersed on the surface of TSO, while the latter shows bigger Pt particles and polydispersion.

Like Pt, Au nanoparticles were uniformly dispersed on TSO under pH=2 (Fig.1e), while it was

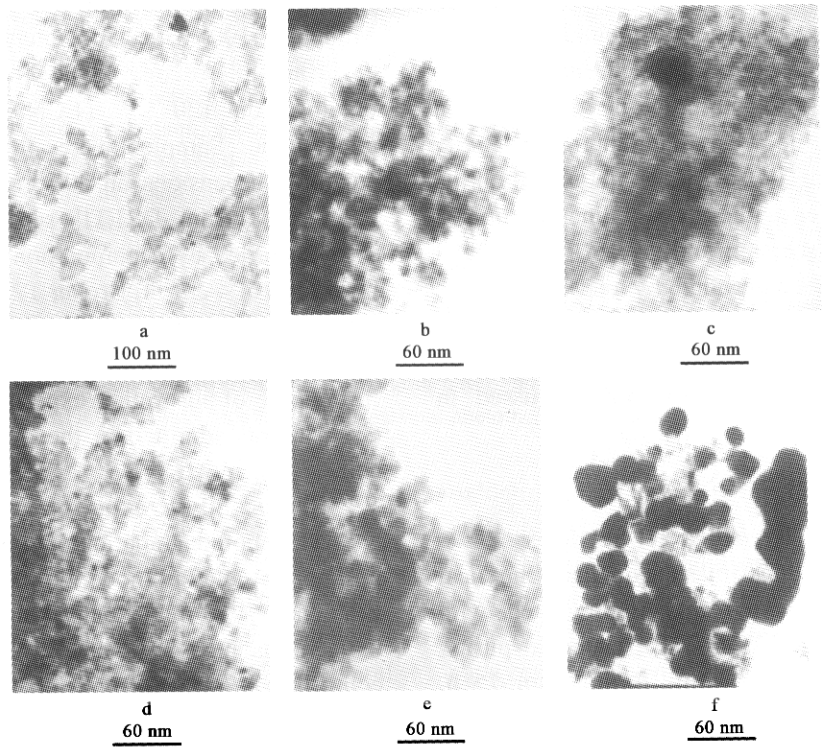

Fig.1 TEM images of Pt-TSO prepared under pH =2 (a), pH = 6.58 (b), Pd-TSO prepared under pH = 2 (c), pH = 9.9 (d), Au-TSO prepared under pH = 2 (e) and pH = 6.58 (f)

disorderly disposed on TSO with metal islands under pH=6.58 (Fig.1f). The main reason is that the both precursor ions are anions $PtCl_6^{2-}$, $AuCl_3$ $(OH)^-$. Fig.1d shows that Pd was uniformly photodeposited on TiO_2 of TSO prepared under pH =9.9, while the surface of Pd-TSO(pH = 2) has Pd particles aggregation in Fig.1c due to Pd precursor ion Pd^{2+}. These results indicate that the pH of solution have strong effect on dispersion, size and sites of metal nanoparticles on TSO. It is known that the surface charge and the adsorptivity of metal-containing ions are highly influenced by the pH of the suspension. This phenomenon can also be used to control the local concentration of metal-containing ions on the surface and the nucleation kinetics for the deposition of metal cluster(Ohtani *et al.*, 1987).

In photodeposition process, two steps were involved (shown in the following equations). In the first step, precursor anions or cations containing metal were adsorbed to the surface of TSO via electrostatic binding, which determined the dispersion and sites of metal on the surface of TSO. In the second step, adsorbed metal ions were photoreduced, which determined the chemical state of metal.

$$TiO_2/\text{silica gel} + h\nu \longleftrightarrow e^- + h^+ \quad (h\nu > E_{bg}) \qquad (1)$$

$$H_2O \longleftrightarrow H^+ + OH^- \qquad (2)$$

$$OH^- + h^+ \longrightarrow OH^{\cdot} \qquad (3)$$

$$M_{ad} + e^- \longrightarrow M' \qquad (4)$$

$$aM' \longrightarrow M_a' \qquad (5)$$

Where M_{ad} refers to the adsorbed ions containing metal, M' refers to metal. The metal can be uniformly deposited on TSO only when the photogenerated electron reacted with the adsorbed ions. Otherwise, the reaction of electron with the metal-containing ions in solution would result in the aggregation of metal particles. For the chemical structure of TSO, our previous report(Hu *et al.*, 2001) demonstrated that about 78.2% of silanol groups on the silica gel surface linked to titanol group, while about 21.8% silanol groups remained on the silica surface. Therefore, the surface groups of TSO seem to be predominant titanol group. The electron point of

TiO_2/silical gel is pH=3, which was shown in the previous paper. The TiO^- groups were predominant on the surface of TSO photocatalyst in pH>3 solution, whereas the $TiOH_2^+$ groups were predominant in pH<3 solution. Under pH =2 condition, Pt and Au would be uniformly photodeposited on the titanol site of TSO by the electrostatic binding of $HPtCl_6^-$ or $AuCl_3(OH)^-$ and $TiOH_2^+$, at pH=6.58, they would be disorderly photodeposited on the titanol and silanol groups due to the repulsive electrostatic power between the negatively charged surface (TiO^-) and $HPtCl_6^-$ or $AuCl_3$ $(OH)^-$ and subsequently accumulated to metal islands on TSO. The metal islands could grow rapidly and sometimes overshadowed the original TiO_2 particles(20 nm) of TSO(Hu, 2001). On the contrast, at pH=9.9, Pd would be orderly photoreduced on the titanol site of TSO by the electrostatic binding of Pd^{2+} and TiO^- while Pd would be disorderly photodeposited on the titanol or silanol groups by the repulsive electrostatic power between $TiOH_2^+$ and Pd^{2-} at pH=2 where $TiOH_2^+$ is predominate groups on TSO. Fig.2a shows that Pt-TSO (pH=2) has bigger visible absorption than Pt-TSO (pH=6.58), while Pd-TSO (pH=9.9) has much stronger absorption than that one prepared under pH=2 in visible light (Fig.2b). According to these reports (Alvarez *et al.*, 1997; Mirkin *et al.*, 1996), this results also indicate that Pt, Pd much more photodeposited on TSO under pH=2, pH=9.9 respectively, further verifying the deposition sites of noble metal on TSO could be controlled by electrostatic binding. UV-Vis DRS spectra of Au-TSO (Fig.2c) shows that Au-TSO prepared under pH=6.58 presents a broad band of 520—530 nm, and Au-TSO prepared under pH=2 has no sharp absorption. The result indicates that the former nanoparticles are bigger than 5 nm (Henglei and Meisel, 1998), and the latter nanoparticles are smaller than 5 nm.

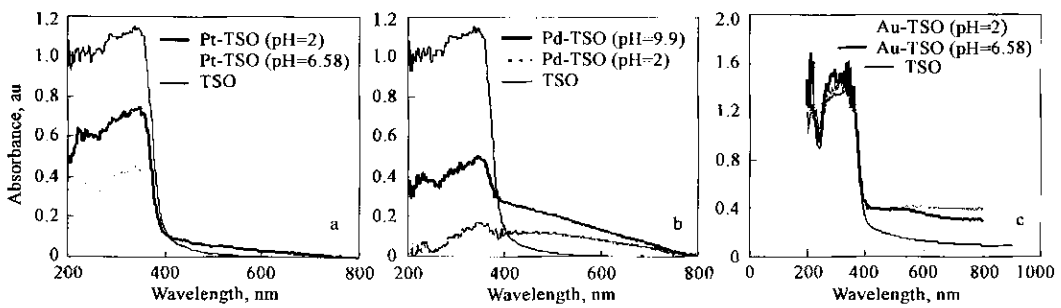

Fig.2 UV-Vis diffuses reflectance spectra of Pt-TSO(a), Pd-TSO(b) and Au-TSO(c) prepared under different pH conditions

2.2 Photothermal catalytic activity of M-TSO

2.2.1 Effects of pH

Fig.3a shows the conversion of ethylene under different temperature by Pt (0.5%)-TSO prepared at pH=2 and pH=6.58, respectively. The final conversion ratio of ethylene is 100% and reaction equilibrium needs about 3 min using the former catalyst, while the final ratio is 80% and reaction equilibrium needs about 40 min using the latter one. The reaction of ethylene conversion is performed at temperature 363 K, UV-illuminated conditions. Photocatalytic oxidation and thermal catalytic oxidation contribute to the conversion rate of ethylene. A significant photothermal synergistic effect was observed in all experiments, which will be verified in the following section. Similarly, 0.5% Au-TSO prepared under pH=2 shows higher photothermal catalytic activity than that one made under pH=6.58(Fig.3b). Compared with different TEM results of these catalysts, the results indicate that the smaller size and better dispersion of metal clusters on TSO could achieve the higher photothermal synergistic effect. In addition, Au-TSO shows significant photothermal synergistic effect at temperature 403 K whereas Pt-TSO appears the role at temperature 363 K. The result reveals that the thermal activity of Au is lower than that one of Pt at the same supporter of TSO. However, the effect of preparing solution pH on their activities is the same due to similar precursor ions. Contrarily, the Pd-TSO prepared under pH=9.9 exhibits much higher activity than that one prepared under pH=2. Using the former catalyst, the final conversion ratio of ethylene is 100% and the equilibrium needs several minutes, whereas under the latter catalyst, the final conversion is 60% the equilibrium needs about 60 min shown in Fig.3c. However, the conversion of ethylene decreased at pH 12.16(Fig.3c). The results agree with that one of TEM. An obvious direct impact of pH on the system is its dispersion quality. To obtain a well-dispersed TSO system, the initial pH of the suspension should be away from the isoelectric point of TSO (3.0). The pH employed not only should ensure the Pd^{2+} to be

adsorbed onto the surface of TSO and receive electrons from the reduction sites, but also should be in the range that allows such effective surface adsorption and prevents Pd^{2+} from precipitation. At extremely low pH, the TSO surface can be so positively charged that surface adsorption of Pd^{2+} becomes very little even inefficient. At pH 12.16, Pd^{2+} could form PdO to deposit on TSO, resulting in a decrease of photothermal oxidation of ethylene.

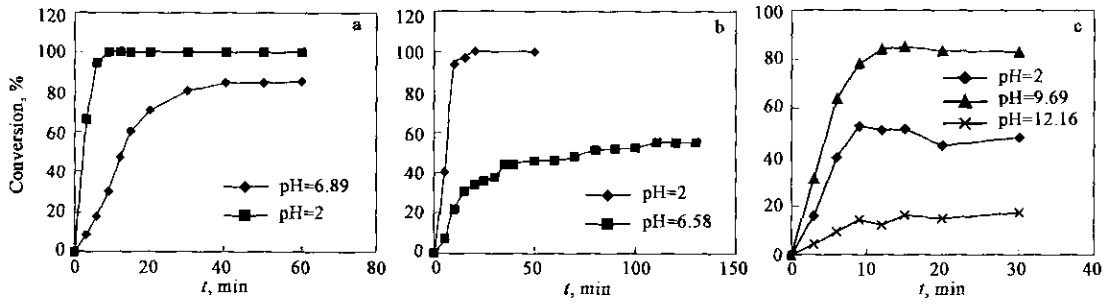

Fig.3 The photothermal oxidation conversions of ethylene under Pt-TSO(a) temperature: 363 K; Au-TSO (b) temperature: 403 K; Pd-TSO(c) temperature: 363 K with UV illumination

2.2.2 Effect of light intensity

Fig.4 shows the conversion of ethylene with two catalysts prepared at different light intensity. Clearly, the photothermal catalytic activity of the catalyst increased with the light intensity decreasing. The rates of photoreduction and photodeposition of metal ions increased with light intensity increasing. Therefore, the bigger photodeposition rate could cause metal particles polydispersion, whereas the slower photodeposition rate could lead to the smaller nanometer size and better dispersion. Only nanoparticles have special catalytic activity, so the Pt-TSO prepared under 4 W light illumination shows higher photothermal synergistic effect.

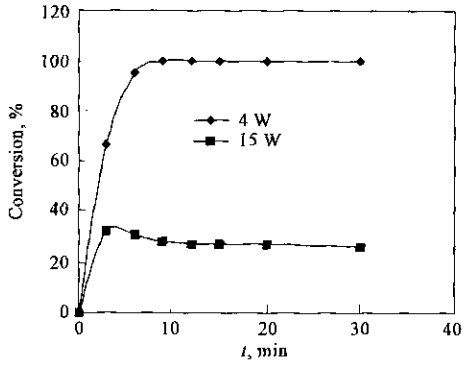

Fig.4 The photothermal catalytic oxidation of ethylene under Pt-TSO prepared from different light intensity(363 K)

2.2.3 Effects of metals weight loading

The weight loading of noble metals is also crucial factor for metal dispersion and size on TSO, leading to different photoactivities. Fig.5a shows 0.25wt% Pt-TSO has maximum photoefficiency than 0.5 wt% and 1 wt% Pt-TSO for ethylene photooxidation. This result indicates that 0.25 wt% sample has the best dispersion and smaller nanometer size, while Au-TSO (Fig.5b), the optimal loading amount is 0.5 wt % Au, which corresponds to the best dispersion and nanometer size. Fig.6 shows the size of Au nanoparticles on TSO grow bigger with the loading amount increasing because the bigger particle can occur stronger plasmon absorption. 1.5% Au-TSO shows significant absorption in 520—530 nm visible region, indicating the Au nanoparticles size more than 50 nm. For Pd-TSO (Fig.5c), the optimal loading amount is 1 wt% Pd corresponding to the best dispersion and nanometer size. The palladium precursor ions are Pd^{2+}. It holds smaller space than $PtCl_6^{2-}$, $AuCl_3$ $(OH)^-$ do, leading to the greater loading amount for highly dispersion. As the metal loading amount increase, the dispersion decrease, the metal particles grow bigger and become recombination of electron-hole to decrease photoefficiency. The bigger metal particles would miss their special optical and catalytic properties, which unusually depended on the particle size(Mulvaney,1996; Heath *et al.*, 1997).

2.2.4 Effect of temperature with metal-modified TSO

Using GC/catalytic conversion furnace/FID, ethylene and the production of carbon dioxide were monitored to calculate a mass balance. The results indicated that the ethylene was completely mineralized to carbon dioxide and water. In addition, no other peaks were detected with GC/FID. The degradation of ethylene was also investigated in an initially dry feed stream at three different temperatures (333 K, 363 K, 403 K) with different catalysts in the presence of UV light. Percentage of total conversion

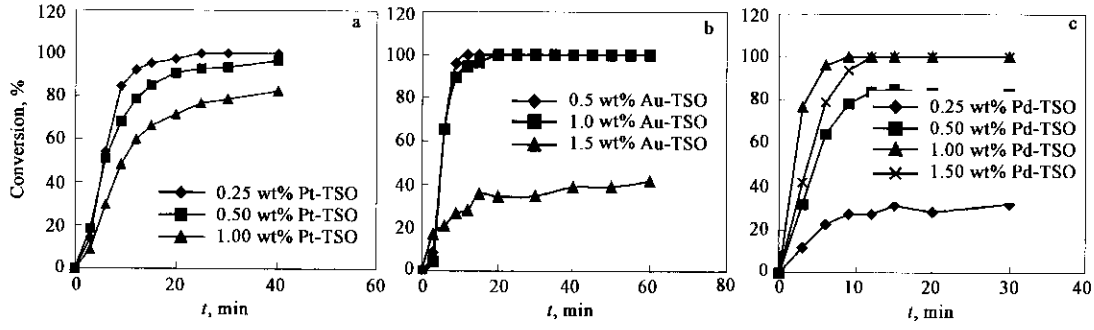

Fig.5 The effects of different loading weight on the photothermal activity of Pt-TSO(a), Au-TSO(b) and Pd-TSO(c) for ethylene oxidation

of ethylene and percentage of conversion to CO_2 were used to compare PCO and catalytic oxidation at different temperatures, as listed in Table 1. As with TSO catalyst, the conversion of ethylene and production of CO_2 are not significantly changed with temperatures increasing, and no catalytic oxidation is observed at three tested temperatures. Pt-TSO, Pd-TSO, Au-TSO also did not exhibit significant catalytic oxidation performance at 333 K. The results agreed with previous report, the activation energies for the heterogeneous catalytic oxidation of ethylene was 82.8 kJ/mol(Fu *et al.*, 1996). However, with temperature increasing, the dark activity of the three catalysts significantly increased. The activity for the ethylene removal and the CO_2 production over illuminated metal (Pt, Pd, Au) -TSO is much greater than the sum of the illuminated TSO and dark metal (Pt, Pd, Au) -TSO. The enhanced ethylene removal and the CO_2 production become more apparent at 403 K. The results of conventional heterogeneous catalysis alone (in dark) are shown in table1 at three temperatures with (Pt, Pd, Au) -TSO. Although the conventional catalysis occurs to some degree at above 333 K, the addition of UV light greatly enhances the oxidation of ethylene to carbon dioxide and water.

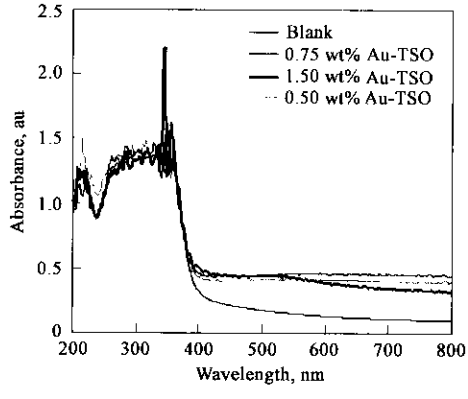

Fig.6 UV-Vis diffuse reflectance spectra of Au-TSO with different Au loading weight

Table 1 Percentage of conversion of ethylene and CO_2 under different reactin conditions Unit: %

Catalyst	333 K		363 K		403 K	
	C_2H_4	CO_2	C_2H_4	CO_2	C_2H_4	CO_2
TSO[a]	22.1	20	23	20	28	20
TSO[c]	-	-	3.7	-	5.7	-
Pt-TSO[a]	30	30	100	100	100	100
Pt-TSO[c]	-	-	34	18	100	80
Pd-TSO[a]	29	28	100	74.6	100	100
Pd-TSO[c]	-	-	19.2	4.3	91.7	56
Au-TSO[a]	25.6	21.6	94.9	94	100	100
Au-TSO[c]	-	-	4.5	3.0	55.6	43.2

Notes: a. Photocatalytic oxidation; c. catalytic oxidation

2.3 FTIR study of metal-modified TSO

In order to monitor the changes in the surface composition during the photocatalytic oxidation of ethylene, A FTIR study of 0.5% Pd/TSO, 0.25% Pt/TSO samples in both fresh and used conditions was undertaken. The modification of platinum, palladium particles under these conditions was investigated by CO adsorption. Fig.7 displays the FTIR spectra of 0.25% Pt/TSO obtained in the 2200—1200 cm^{-1} rang spectrum. In the case of the fresh sample the spectrum (Fig.7A, dashed line) shows four main bands that can be assigned to water (1626 cm^{-1}; bending mode) and adsorbed carbonates and/or acetates at 1445 cm^{-1}, Following CO adsorption (3% CO, balance gas nitrogen) and equilibration for 2 h(Fig.7B, solid line), new bands develop, which correspond to CO adsorbed on-top (2112 and 2089 cm^{-1}), on line sites of Pt^0 particles. The IR spectrum of the used 0.25% Pt/TSO is almost the same as the fresh one. Fig.8 also shows the common IR spectrum of the both fresh and used 0.5% Pd/TSO. The new bands corresponding to CO adsorbed on-top(2090, 2107 cm^{-1}), on line sites of Pd^0 particles. The results indicate that the products of the photo-oxidation of ethylene do not accumulate on the surface of the catalysts in the course of the reaction. The 0.25% Pt/TSO did not show any activity decrease

after it was used for more than 100 h. The introduction of noble metals leads to photothermal synergism to enhance the selectivity of CO_2 production to decrease the accumulation of intermediates and prevent deactivation of the catalyst.

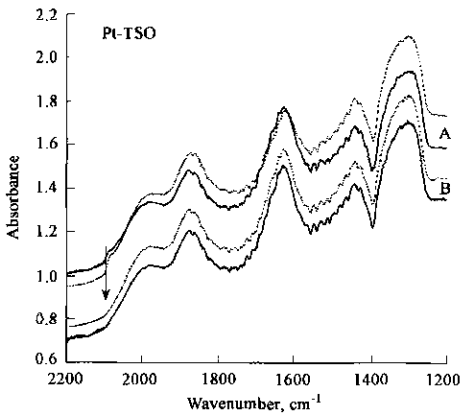

Fig.7 FTIR spectra of the sample 0.25%Pt/TSO fresh (A) and used for the photothermal catalytic oxidation of ethylene (B) purged with high purity nitrogen at 373 K for 2 h (dashed line) and following admission of 3%CO(solid line)

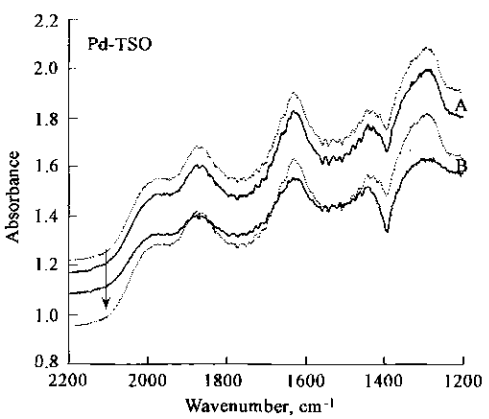

Fig.8 FTIR spectra of the sample 0.5% Pd/TSO fresh(A) and used for the photothermal catalytic oxidation of ethylene (B) purged with high purity nitrogen at 373K for 2h (dashed line) and following admission of 3% CO (solid line)

3 Conclusions

The dispersion, size and sites of metal nanoparticles supported on TSO could be controlled via electrostatic binding of metal ions and TiO^- or $TiOH_2^+$ by adjusting pH of solution. Under appropriate pH conditions, metal nanoparticles were uniformly photodeposited on TSO. The characterization of UV-Vis DRS, TEM, indicated the effects of pH, loading weight, and light intensity on the morphology of metal nanoparticles on TSO during photocatalytic deposition. The uniform dispersion, smaller nanosize could produce the higher photothermal catalytic efficiency for ethylene oxidation. The synergism of metal nanoparticles catalysis and TSO photocatalysis enhances the ethylene removal and the production of CO_2, and avoid the accumulation of by-product on the surface of the catalyst indicated by FTIR analyses.

References:

Alberici R M, Jardim W F, 1995. Photocatalytic destruction of VOCs in the gas-phase using titanium dioxide[J]. Appl Catal B, 14: 55—68.

Alvarez M M, Khoury J T, Schaaff T G *et al.*, 1997. Optical absorption spectra of nanocrystal gold molecules [J]. J Phys Chem B, 101 (19): 3706—3712.

Ameen M M, Raupp G B, 1999. Reversible catalyst deactivation in the photocatalytic oxidation of dilute *o*-xylene in air[J]. J Catal, 184: 112—122.

Das D, Lee J F, Cheng Soofin, 2001. Sulfonic acid functionalized mesoporous MCM-41 silica as a convenient catalyst for Bisphenol-A synthesis[J]. Chem Commun, 1(21): 2178—2179.

Einaga H, Futamura S, Ibusuk T, 2001. Complete oxidation of benzene in gas phase by platinized titania photocatalysts [J]. Environ Sci Technol, 35(9): 1880—1884.

Fu X Z, Zeltner W A, Anderson M A, 1995. The gas-phase photocatalytic mineralization of benzene on porous titania-based catalysts[J]. Appl Catal B, 6: 209—224.

Fu X Z, Clark L A, Walter A *et al.*, 1996. Effects of reaction temperature and water vapor content on the heterogeneous photocatalytic oxidation of ethylene [J]. J Photolchem and Photobiol A: Chem, 97: 181—186.

Fuerte A, Hernó ndez-Alonso, Maira A J *et al.*, 2001. Visible light-activated nanosized deped-TiO_2 photocatalysts [J]. Chem Commun, 24: 2718—2719.

Heath J R, Knobler C M, Leff D V, 1997. Pressure/temperature phase diagrams and superlattices of organically functionalized metal nanocrystal monolayers: The influence of particle size, size distribution, and surface passivant [J]. J Phys Chem B, 101(2): 189—197.

Henglei A I, Meisel D, 1998. Radiolytic control of the size of colloidal gold nanoparticles[J]. Langmuir, 14(26): 7392—7396.

Hu C, Wang Y Z, Tang H X, 2001. Preparation and characterization of surface bond-conjugated TiO_2/SiO_2 and photocatalysis for azo dyes[J]. Appl Catal B, 30: 277—285.

Kennedy J C, Datye A K, 1998. Photothermal heterogeneous oxidation of ethanol over Pt/TiO_2[J]. J Catal, 179: 375—389.

Mirkin C A, Letsinger R L, Mucic R C *et al.*, 1996. A DNA-based method for rationally assembling nanoparticles into macroscopic materials[J]. Nature, 382: 607—609.

Mulvaney P, 1996. Surface plasmon spectroscopy of nanosized metal particles[J]. Langmuir, 12(3): 788—800.

Nosaka Y, Koenuma K, Ushida K *et al.*, 1996. Reaction mechanism of the decomposition of acetic acid on illuminated TiO_2 powder studied by means of *in situ* electron spin resonance measurements[J]. Langmuir, 12(3): 736—738.

Ohtani B, Okugawa Y, Nishimo S T *et al.*, 1987. Photocatalytic activity of titania powders suspended in aqueous silver nitrate solution: correlation with pH-dependent surface structures [J]. J Phys Chem, 91(13): 3550—3555.

Papaefthimiou P, Ioannides T, Verykio X E S, 1998. Performance of doped Pt/TiO_2 (W^{6+}) catalysts for combustion of volatile organic compounds (VOCs)[J]. Appl Catal B, 15: 75—92.

Peral J, Ollis D F, 1992. Heterogeneous photocatalytic oxidation of gas-phase organics for air purification: Acetone, 1-butanol, butyraldehyde, formaldehyde, and m-xylene oxidation[J]. J Catal, 136: 554—565.

Scatter M L, Ross P N, 1986. The surface structure of Pt crystallites supported on carbon black[J]. Ultramicroscopy, 20: 21—28.

Vorontsov A V, Stoyanovl V A, Kozlov D V *et al.*, 1999. Study of TiO_2 deactivation during gaseous acetone photocatalytic oxidation[J]. J Catal, 186: 318—324.

Watanabe M, Sei H, Stonehart P, 1989. The influence of platinum crystallite size on the electrore- duction of oxygen [J]. J Electroanal Chem, 261: 375—387.

Yu J G, Yu J C, Leung Mitch K P *et al.*, 2003. Effects of acidic and basic hydrolysis catalysts on the photocatalytic activity and microstructures of bimodal mesoporous titania [J]. J Catal, 217: 69—78.

Zhang Z C, Beard B C, 1999. Agglomeration of Pt particles in the presence of chlorides[J]. Appl Catal A, 188: 229—240.

Zorn M E, Tompkins D T, Zeltner W A *et al.*, 2000. Catalytic and photocatalytic oxidation of ethylene on titania-based thin-films [J]. Environ Sci Technol, 34(24): 5206—5210.

(Received for review March 23, 2005. Accepted May 27, 2005)